

# A near-infrared spectrometer to measure zodiacal light absorption spectrum

A. S. Kutnyrev<sup>a</sup>, R. Arendt<sup>a</sup>, E. Dwek<sup>b</sup>, R. Kimble<sup>b</sup>, S.H. Moseley<sup>b</sup>, D. Rapchun<sup>d</sup> and R.F. Silverberg<sup>b</sup>

<sup>a</sup>CRESST/UMd/NASA's GSFC, <sup>b</sup>NASA's GSFC, <sup>c</sup>CRESST/UMBS/NASA's GSFC, <sup>d</sup>GST/NASA's GSFC,

## ABSTRACT

We have developed a high throughput infrared spectrometer for zodiacal light Fraunhofer lines measurements. The instrument is based on a cryogenic dual silicon Fabry-Perot etalon which is designed to achieve high signal to noise Fraunhofer line profile measurements. Very large aperture silicon Fabry-Perot etalons and fast camera optics make these measurements possible. The results of the absorption line profile measurements will provide a model free measure of the zodiacal light intensity in the near infrared. The knowledge of the zodiacal light brightness is crucial for accurate subtraction of zodiacal light foreground for accurate measure of the extragalactic background light after the subtraction of zodiacal light foreground. We present the final design of the instrument and the first results of its performance.

**Keywords:** high resolution spectroscopy, Fabry-Perot, zodiacal light, cosmic infrared background, extragalactic background light, airglow

## 1. INTRODUCTION

There is a long history of attempts to measure Fraunhofer line profile in zodiacal light. Starting in early 60-ies of the last century with pioneering attempts<sup>1-3</sup> there were numerous attempts made to observe zodiacal light Fraunhofer spectrum. There were also attempts to approach the problem statistically by measuring multiple underresolved absorption lines.<sup>4</sup> Despite all these efforts it has only recently with the development of new technology and larger aperture high efficiency spectrometers with large Fabry-Perot interferometers, became possible to achieve high signal to noise ratio.<sup>5</sup> This result is very encouraging. It proves the capability of the approach to actually measure the absorption line profile in the zodiacal light spectrum with high spectral resolution.

## 2. SCIENTIFIC GOAL

This spectrometer is being built with the primary purpose of measuring the absolute intensity of the zodiacal light in the J (1.25  $\mu\text{m}$ ) band by measuring Fraunhofer line equivalent width in the zodiacal light spectrum. This method will allow significant improvement in the quality of the foreground subtraction of the COBE DIRBE measurements, largely eliminating the major systematic uncertainty in the DIRBE determination of the near infrared extragalactic background light (EBL).<sup>6</sup> This determination of the near-infrared EBL will be independent of any zodiacal light model. The improved DIRBE zodiacal light model will provide a first measurement of the EBL and therefore will have significant impact on related cosmological questions, such as massive primordial star formation and energy releases throughout cosmic history.

---

Further author information: (Send correspondence to A.K.)

A.K.: E-mail: [alexander.kutnyrev@nasa.gov](mailto:alexander.kutnyrev@nasa.gov), Code 665, NASA/GSFC, Greenbelt, MD20771

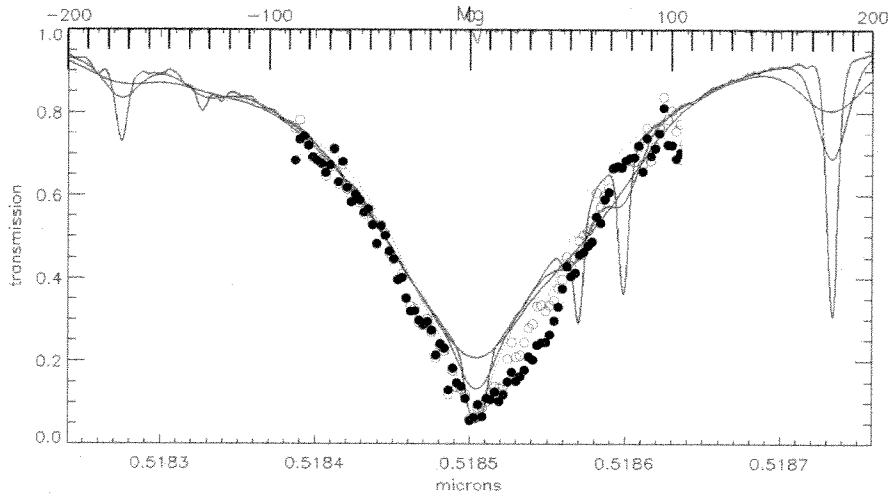


Figure 1. Zodiacal light MgI 5184 Å Fraunhofer line observed using large aperture WHAM (Wisconsin H-Alpha Mapper) Fabry-Perot spectrometer<sup>5</sup>. The dots are observed data, solid lines are solar spectrum without broadening and with 25km/s and 50 km/s Gaussian broadening to simulate broadening caused by scattering on zodiacal cloud particles.

### 3. OBSERVATIONAL CHALLENGE AND PROPOSED SOLUTION

To accurately measure the brightness of the zodiacal light from the ground based observatory using Fraunhofer lines we must have: (1) a clear understanding and separation of the sources contributing to the spectrum; (2) evaluate the contribution of these sources; and (3) design a spectrometer that would provide the highest possible signal to noise ratio of the observed lines. Although measuring the equivalent width of the absorption line allows to separate featureless continuum from the absorption spectrum, the spectra also contain the contribution from stellar sources that have similar spectral features. We therefore have to take measures to eliminate or reduce their effects on the result at every step: at the instrument design, observing procedure, and at the analysis stage.

#### Atmospheric emission lines and continuum

The spectrum of the diffuse component of the sky background in the near infrared is quite complex and comprises multiple components. The primary contributors to the continuum emission are zodiacal light, the Earth atmospheric emission and stellar continuum.<sup>7</sup> The primary source of atmospheric emission in the infrared is hydroxyl airglow. These lines originate in the upper atmosphere and result from the photochemical reactions. They have diurnal variations and can vary on time scales of minutes.<sup>8</sup> The effect on the astronomical spectroscopy results are very severe, thus these lines have been a subject of extensive studies in astronomical and geophysical research<sup>9-11</sup>. To reduce the adverse effects by these emission lines we searched for regions in spectrum that are free from these emission lines. Due to extremely large number of emission lines and telluric lines in atmospheric spectrum it is not easy, but possible since our spectral range is narrow (only  $10^{-3}\lambda$ ) and we had a freedom of choice of the Fraunhofer line selection in the zodiacal light spectrum. We are looking for a line (or lines) that would be strong and free from the atmospheric emission of absorption features.

One of the consequences of very intense hydroxyl emission in the near infrared combined with their pervasiveness is that the brightness of the airglow continuum is not well known. It has not been measured primarily because of the weakness of continuum that is hidden underneath of the bright hydroxyl emission lines. The task of measuring this faint continuum emission is virtually impossible since most of the spectroscopic measurements lack high enough spectral resolution and even when they do scattered light in the spectrometer can contaminate the results therefore making it them uncertain. The best results we have found in the literature have an uncertainty of a factor of two to four in the estimate the brightness of the airglow continuum, which is comparable to the brightness of the zodiacal light.<sup>12</sup> Our spectrometer sensitivity estimates are based on these measurements.

#### Stellar background

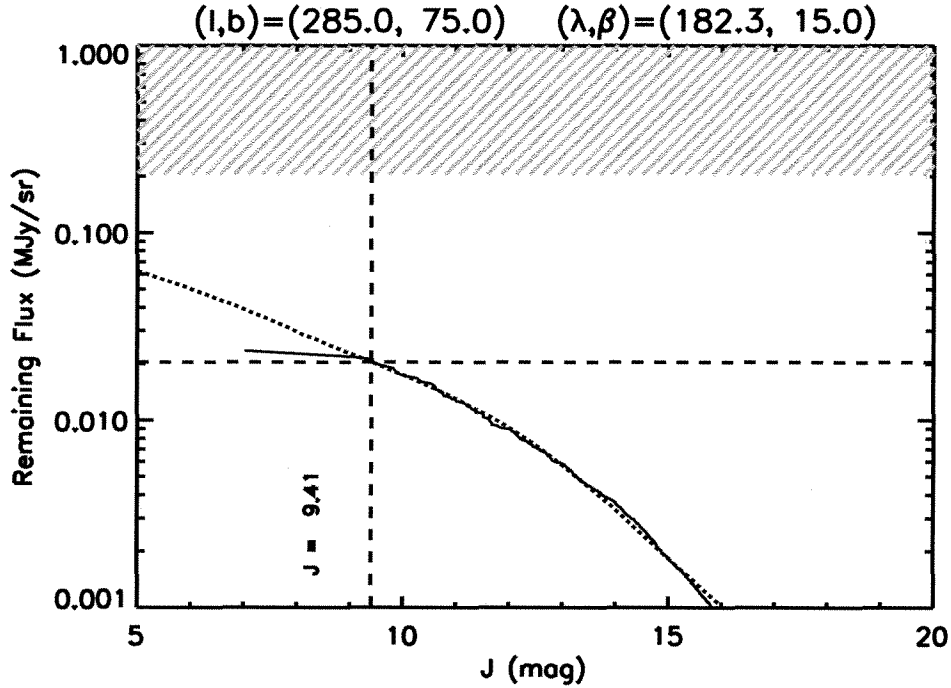


Figure 2. Stellar contribution to diffuse sky brightness depending on the magnitude cut-off. The plot represents remaining stellar brightness in J band above the given magnitude.

To predict the contribution of the unresolved Galactic stellar background to the observed equivalent width of the scattered solar absorption line, we use an implementation of the Wainscoat model<sup>13</sup> of the Galactic stellar population combined with the Coelho library<sup>14</sup> of synthetic stellar spectra. This model allows us to estimate the residual stellar contribution to the J band intensity when stars brighter than some given magnitude are masked out. The process is illustrated for a line of sight at a relatively high galactic latitude and low ecliptic latitude. The solid black line (Fig. 2) shows the model prediction of the total residual intensity remaining as a function of the cut-off magnitude. The red line shows the result derived from 2MASS point source counts in a 1 square degree region at this location. The agreement is good (within 10%) in the range where the 2MASS counts are unaffected by either incompleteness or small number statistics. The blue shaded region (upper part of the plot) indicates the possible range of brightness of the zodiacal light, which depends on the solar elongation. The maximum zodiacal light is off scale at 2 MJy/sr at solar elongation of  $\sim 60^\circ$ . If we impose a criterion that the unmasked starlight should be no brighter than e.g. 0.1 times the minimum zodiacal light intensity (horizontal dashed line), then both the model and the 2MASS data indicate that we need to mask all stars brighter than 9.41 magnitude (vertical dashed line).

We modeled the contribution of the intensity contributed by each of the different components of the model, when stars brighter than 9.41 magnitude are masked. That was done to compare the integral spectrum background stars fainter than the selected cut-off magnitude to the solar spectrum. The bulk of the remaining starlight is from late-F through M main sequence stars in the Galactic disk. The contributions from red giant stars (especially in the disk) and early type stars is greatly reduced because these intrinsically bright stars are mostly rejected by the masking process. The spectrum of these stars is similar to the solar spectrum, which makes it hard to separate them spectrally, especially considering the poorly known velocity dispersion of these stellar populations. Therefore masking the stars out is an important part of the observation technique.

### Spectral line selection

The line selected for observations must be free of contamination by telluric absorption and atmospheric emission lines. To achieve the best results the line should be deep and has equivalent width of 20 km/s - 40

km/s, which is close to the zodiacal light line width caused by the differential motion of the zodiacal dust cloud. We have modeled the spectra using solar and telluric lines spectra. The result of the model for two selected spectral lines is presented in Fig. 3. These lines were also selected for absence of the bright hydroxyl lines in the vicinity of the selected range. The effects of these faint spectral features will be accounted for by doing calibration and at different elevation and at different time of night. But despite all the care taken in the line selection and calibration efforts there still might be some residual effects of these varying atmospheric mission lines.<sup>5</sup> To make the results of the study more robust and evaluate the systematic effects we will observe in two separate lines. It will greatly improve confidence of the obtained results and will help eliminate any issues related to the faint variable atmospheric lines.

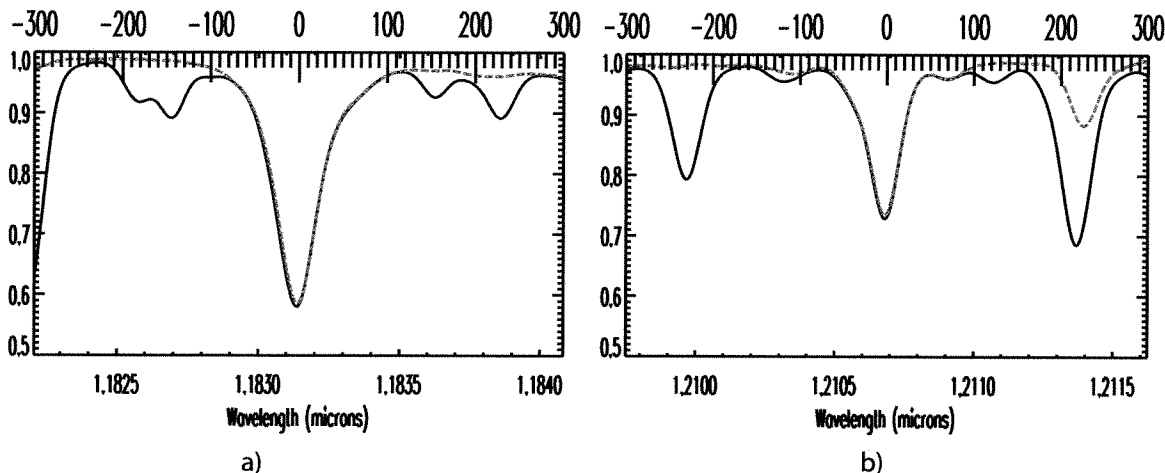


Figure 3. Modeled spectra of the selected zodiacal lines. Two stronger lines were selected in the solar spectrum to avoid bright airglow emission lines and telluric lines: a) Mg I 11828.19  $\mu\text{m}$  and b) Si I 12103.54  $\mu\text{m}$ <sup>15</sup> (wavelength values are in air). These lines are relatively strong and narrow, are not blended with other solar lines and free of atmospheric emission lines and telluric lines. The dashed line is pure zodiacal light spectrum; solid line is expected real spectrum with zodiacal and telluric lines.

#### 4. SPECTROMETER DESIGN

The selection of the spectrometer type was dictated by the need of highest achievable étendue of the instrument for a given spectral resolving power of  $2 \times 10^4$ . We selected the Fabry-Perot spectrometer after careful comparison of the best candidates, such as Fourier transform spectrometer, spatial heterodyne spectrometer<sup>16</sup> and Fabry-Perot etalon based spectrometer. Our decision was based on the achievable accuracy with the practical consideration for the time scale for building the instrument.

The general outline of the instrument is shown in Fig. 4. The core of the spectrometer is comprised of two etalons and a narrow band filter that suppresses the etalons out of band transmission orders. The front optics of the instrument includes a 30 cm diameter Cassegrain telescope with the re-imaging lenses and focal plane mask that allows to block the bright stars in the field of view. A folding mirror and a CCD camera are used to obtain an image of the bright stars in the focal plane and manufacture a mask that is placed in the focal plane to block these stars. The Cassegrain focal plane is re-imaged onto the etalons assembly inside the liquid nitrogen dewar that accommodates the spectrometer itself, including a narrow band interference filter, both etalons, the camera lens assembly and the detector. The etalons are tuned to the same wavelength by changing their temperature. The refractive index thermal coefficient of silicon is high enough that a change of 30-40K in temperature.<sup>17</sup> An image of the system pupil is produced onto a 1024x1024 HgCdTe HST WFC3 detector.<sup>18</sup> The spectrometer operates in non-imaging integral mode, where all objects in its field of view contribute to each spectral element equally. The full spectrum is obtained in a single acquisition, which increases the efficiency proportionally to the number of spectral elements in the spectrum. The spectral resolution of the instrument should provide Nyquist

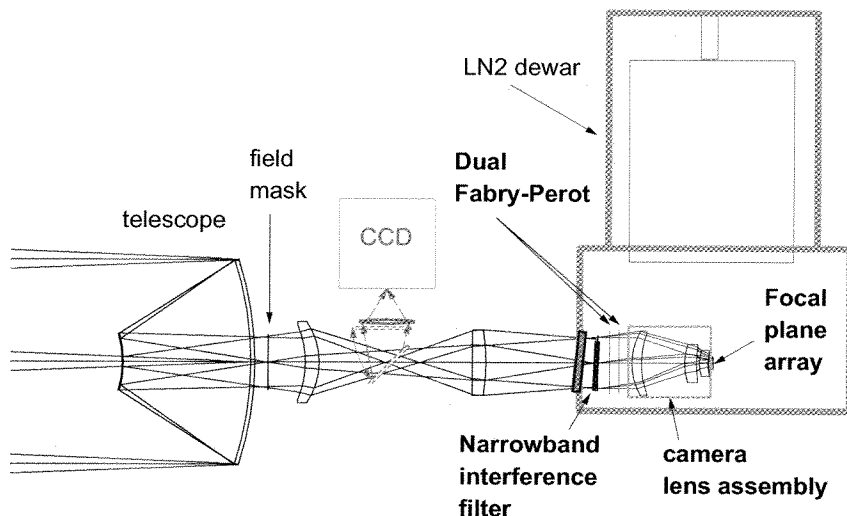


Figure 4. Zodiacal light spectrometer layout.

sampling of the spectrum or somewhat higher to enable kinematic studies of the zodiacal light. The expected line width of the zodiacal light Fraunhofer line is 20-40 km/s. The line selected spectral resolution of 15 km/s will provide 1-3 times Nyquist sampling of the line. At this spectral resolution and 400 km/s spectral range there will be 26 spectral element in the spectrum. Various aspects of the individual components of the system are described in this section.

#### 4.1 Etalons.

To achieve the highest possible detection limit of the absorption features in the zodiacal light spectrum we use dual Fabry-Perot interferometer. We decided to use solid etalons made out of silicon which will provide a very compact high throughput spectrometer, that exceeds in its throughput any other available etalons. Our previous solid etalon development<sup>17</sup> proved the feasibility of this approach. The throughput of solid etalon is larger than the conventional vacuum or gas gap etalon is proportional to the square of the material refractive index. With the silicon refractive index as high as 3.4, the throughput increases by more than an order of magnitude. That makes solid etalon very appealing for such demanding applications as low brightness diffuse extended sources.

Since etalons are inherently low contrast devices and our task is to detect absorption line on a relatively high continuum background, the spectrometer should be a dual etalon instrument. The etalons that are being fabricated by Light Machinery Inc. have a 75 mm clear aperture. These etalons are equivalent to a vacuum gap etalon of  $\sim 20$ cm diameter. The high temperature coefficient of silicon refractive index will allow to tune the etalons thermally by moderate change in the etalon temperature. By adjusting the temperature of each etalon the spectrometer transmission will be tuned, so that the line of interest is positioned in the centre of the spectral range. A narrow band ( $\sim 0.4\%$  FWHM) will suppress etalons spectral transmission sidelobes. With the narrow band pre-filter and two selected etalons in series we can achieve a good rejection and lower the contribution of noise from the out of band parasitic transmission.

Once the etalons are tuned to the desired wavelength they are kept stable at that temperature. There is no spectral scanning in the system since the whole spectrum is acquired simultaneously. To achieve the highest possible étendue we decided to utilize multiple ring integration technique employed by Wisconsin H-

alpha Mapper dual Fabry-Perot spectrometer<sup>19</sup> that allows simultaneous detection of the whole spectrum, using spectral multiplicity advantage.

## 4.2 Optical system

The most efficient configuration of the Fabry-Perot spectrometer for observing extended diffuse objects is a non-imaging mode, when the spectrometer interference pattern is overlaid on the system pupil and imaged onto the detector. With this configuration each object in the telescope field of view contributes equally to the detected spectrum. The following data reduction process converts the interferogram image into a spectrum by summing up signal in the equal area rings.

At 400 km/s spectral coverage silicon etalons would have  $17^\circ$  angle field of view on the sky. Though in principle the spectrometer can be used to acquire zodiacal light spectra without any additional front optics, the field of view is too large and also this mode of observing would be prone to fluctuations in the sky brightness (faint clouds, airglow fluctuations etc.) that would produce additional noise that would be hard to account for. A small size feeding telescope would accomplish the goal of making the field uniform (spectrometer is in the pupil imaging mode) and also of reducing the field of view. We selected 30 cm telescope in part for practical reasons, in part because it reduces the field of view to  $4.25^\circ$ , which is small enough to provide adequate sampling of the zodiacal light.

An intermediate focal plane is used to mask out the stars to reduce stellar background on the detector. This is an important part of the system design and observing technique, since stellar background can be comparable to the zodiacal light in brightness and its spectrum is very similar to the zodiacal light spectrum therefore making it very hard to separate them spectrally.

To achieve the best signal to noise ratio for a given detector the image scale should be selected so that the noise would be dominated by the photon noise from the zodiacal light (detector readout noise and dark current noise are negligible). For detectors that are currently available it drives the plate scale to extremely low values requiring extremely fast imaging camera with  $f/\# = 0.35$  which is not achievable in practical design. That scale is close to the smallest scale defined by the interferometer spectral resolution at the narrowest ring. The imaging camera design was the best effort to achieve fastest possible optics that would still provide imaging quality without degrading spectral resolution of the instrument. This imaging requirement is easy to achieve for inner rings of the interferogram, becoming very hard at the edge of the field of view. The camera lens assembly consists of 4 silicon lenses. It has a  $f/0.8$  focal ratio nearly telecentric system that creates a pupil image 20 mm in diameter on the detector.

The results of the this spectrometer capability to detect selected zodiacal light Fraunhofer lines are presented in Fig. 5. The results are presented for an ideal case of photon noise (no detector readout and no dark current), zodiacal light signal on top of atmospheric continuum and a realistic estimate of all the noise sources. As the result demonstrates, a signal to noise ratio of ten can be achieved with an integration time of about hundred seconds. An hour integration time yields a signal to noise ratio of a hundred. This estimate demonstrates that we will be able to acquire multiple fields per observing night, therefore making the survey possible.

We have two filters that are located on the filter wheel that can be changed quickly during the observing. That will enable a ABAB observing sequence when filters A and B will be switching during observations to acquire the data on both A and B filter sequences at about the same conditions (elevation and sky brightness). It is going to be an essential part of the observing process, aimed at reducing systematic effects and achieving the best possible sensitivity. A summary of the spectrometer parameters is given below:

- Silicon double etalon 0.25 mm and 0.3 mm thick
- Clear aperture 75 mm
- Operation mode: pupil imaging
- Temperature change  $\delta T$  required to cover the etalon free spectral range of  $\sim 40K$
- Wavelength 1.182819  $\mu m$  MgI and 1.210354  $\mu m$  and Si I lines (wavelengths in air)

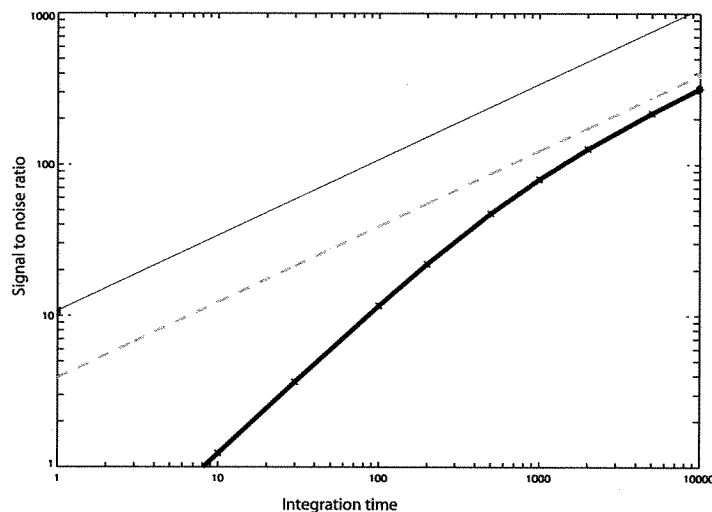


Figure 5. Estimated signal to noise ratio of the instrument for various components of noise versus integration time: thin solid line - zodiacal light photon noise limited performance, dashed line - background continuum, thick black line - signal to noise ratio produced by all the sources, including atmospheric background and detector dark current and readout noise.

- Spectral resolution  $2 \times 10^4$
- Spectral range 400 km/s

### 4.3 Observing.

After we have built and tested the spectrometer in the lab we are planning to conduct when the zodiacal light is bright creating optimal conditions for detecting the selected lines and minimizing the effects of atmospheric spectra. Once these tests are completed, we will have a field trip with the instrument for initial observing run to acquire first batch of data on selected fields. The goal of the first run will be to provide large sky coverage on a significant portion of the ecliptic plane, ecliptic pole and in selected fields at intermediate ecliptic latitudes. This first batch of data should allow us to refine the observing strategy and help to make improvements to the instrument itself if necessary.

The following observing will be done with the adjusted strategy and fields selected on the basis of the initial results. Besides the wide sky coverage we intend to do multiple epoques observations to search for zodiacal light variability discovered by the COBE DIRBE team. The final result of the project should be a (sparse) map of the zodiacal light brightness with kinematic information obtained from the Fraunhofer line profiles. The map can be produced in several stages when at each stage we will acquire a portion of the final map with overlapping with the area observed at the next stage of mapping. The overlap will help to improve the accuracy and to find the variations of zodiacal light brightness with time.

## 5. CONCLUSION

To make the data of the zodiacal light in the J-band along different positions useful for the extended background light measurements we have to measure the equivalent width of the Fraunhofer line with a signal to noise ratio of  $\sim 100$ . Our models of the expected instrument sensitivity show that this level of accuracy can be achieved in a single exposure of 1000 - 3000 seconds integration. To map the zodiacal light and measure possible variations we will select and observe multiple fields and carry out the measurements at several epoques. Observing at multiple epoques will allow to improve accuracy and to measure annual variations of the zodiacal light brightness. Besides the equivalent width measurements for EBL these results will be a powerful tool for zodiacal dust cloud modeling.

## ACKNOWLEDGMENTS

We greatly appreciate Randy Kimble, Bob Hill and HST WFC3 team for support in acquiring the detector and with various aspects of the detector electronics. We acknowledge support of this project by NASA though APRA funding.

## REFERENCES

1. N. K. Reay and J. Ring, "Radial Velocity Measurements on the Zodiacal Light Spectrum," *Nature* **219**, pp. 710–+, Aug. 1968.
2. N. K. Reay and J. Ring, "Radial velocity and intensity measurements of the night sky H-beta emission line," *Planet. Space Sci.* **17**, pp. 561–+, Mar. 1969.
3. I. R. East and N. K. Reay, "The motion of interplanetary dust particles. I - Radial velocity measurements on Fraunhofer line profiles in the Zodiacal Light spectrum," *A& Ap* **139**, pp. 512–516, Oct. 1984.
4. R. A. Bernstein, W. L. Freedman, and B. F. Madore, "The First Detections of the Extragalactic Background Light at 3000, 5500, and 8000 Å. II. Measurement of Foreground Zodiacal Light," *ApJ* **571**, pp. 85–106, May 2002.
5. R. J. Reynolds, G. J. Madsen, and S. H. Moseley, "New Measurements of the Motion of the Zodiacal Dust," *ApJ* **612**, pp. 1206–1213, Sept. 2004.
6. M. G. Hauser, R. G. Arendt, T. Kelsall, E. Dwek, N. Odegard, J. L. Weiland, H. T. Freudenreich, W. T. Reach, R. F. Silverberg, S. H. Moseley, Y. C. Pei, P. Lubin, J. C. Mather, R. A. Shafer, G. F. Smoot, R. Weiss, D. T. Wilkinson, and E. L. Wright, "The COBE Diffuse Infrared Background Experiment Search for the Cosmic Infrared Background. I. Limits and Detections," *ApJ* **508**, pp. 25–43, Nov. 1998.
7. C. Leinert, S. Bowyer, L. K. Haikala, M. S. Hanner, M. G. Hauser, A.-C. Levasseur-Regourd, I. Mann, K. Mattila, W. T. Reach, W. Schlosser, H. J. Staude, G. N. Toller, J. L. Weiland, J. L. Weinberg, and A. N. Witt, "The 1997 reference of diffuse night sky brightness," *A&ApS* **127**, pp. 1–99, Jan. 1998.
8. H. U. Frey, S. B. Mende, J. F. Arens, P. R. McCullough, and G. R. Swenson, "Atmospheric gravity wave signatures in the infrared hydroxyl OH airglow," *GRLet* **27**, pp. 41–44, 2000.
9. P. Rousselot, C. Lidman, J.-G. Cuby, G. Moreels, and G. Monnet, "Night-sky spectral atlas of OH emission lines in the near-infrared," *A& Ap* **354**, pp. 1134–1150, Feb. 2000.
10. S. K. Ramsay, C. M. Mountain, and T. R. Geballe, "Non-thermal emission in the atmosphere above Mauna Kea," *MNRAS* **259**, pp. 751–760, Dec. 1992.
11. E. Oliva and L. Origlia, "The OH Airglow Spectrum - a Calibration Source for Infrared Spectrometers," *A& Ap* **254**, pp. 466–+, Feb. 1992.
12. T. Maihara, F. Iwamuro, T. Yamashita, D. N. B. Hall, L. L. Cowie, A. T. Tokunaga, and A. Pickles, "Observations of the OH airglow emission," *PASP* **105**, pp. 940–944, Sept. 1993.
13. R. J. Wainscoat, M. Cohen, K. Volk, H. J. Walker, and D. E. Schwartz, "A model of the 8-25 micron point source infrared sky," *ApJSS* **83**, pp. 111–146, Nov. 1992.
14. P. Coelho, "Model stars for the modelling of galaxies:  $\alpha$ -enhancement in stellar populations models," *ArXiv e-prints* **802**, Feb. 2008.
15. J. Meléndez and B. Barbuy, "Oscillator Strengths and Damping Constants for Atomic Lines in the J and H Bands," *ApJSS* **124**, pp. 527–546, Oct. 1999.
16. F. L. Roesler, J. M. Harlander, J. G. Cardon, C. R. Englert, R. J. Reynolds, K. Jaehnig, S. Watchorn, E. J. Mierkiewicz, and J. Corliss, "Spatial Heterodyne Spectroscopy: An Emerging Technology for Interference Spectroscopy," in *Hubble's Science Legacy: Future Optical/Ultraviolet Astronomy from Space*, K. R. Sembach, J. C. Blades, G. D. Illingworth, and R. C. Kennicutt, Jr., eds., *Astronomical Society of the Pacific Conference Series* **291**, p. 395, 2003.
17. A. S. Kutyrév, C. L. Bennett, S. H. Moseley, D. Rapchun, and K. P. Stewart, "Near infrared cryogenic tunable solid Fabry-Perot spectrometer," in *Ground-based Instrumentation for Astronomy. Edited by Alan F. M. Moorwood and Iye Masanori. Proceedings of the SPIE, Volume 5492, pp. 1172-1178 (2004).*, A. F. M. Moorwood and M. Iye, eds., *Presented at the Society of Photo-Optical Instrumentation Engineers (SPIE) Conference* **5492**, pp. 1172–1178, Sept. 2004.



18. R. A. Kimble, J. W. MacKenty, and R. W. O'Connell, "Status and performance of HST/Wide Field Camera 3," in *Space Telescopes and Instrumentation I: Optical, Infrared, and Millimeter*. Edited by Mather, John C.; MacEwen, Howard A.; de Graauw, Mattheus W. M.. *Proceedings of the SPIE, Volume 6265*, pp. 62650I (2006)., Presented at the Society of Photo-Optical Instrumentation Engineers (SPIE) Conference **6265**, July 2006.
19. R. J. Reynolds, S. L. Tufte, L. M. Haffner, K. Jaehnig, and J. W. Percival, "The Wisconsin H-alpha Mapper (WHAM): A brief review of performance characteristics and early scientific results," *Publications of the Astronomical Society of Australia* **15**, pp. 14-18, Apr. 1998.